Talanta 81 (2010) 438–443

Contents lists available at ScienceDirect

Talanta

journal homepage: www.elsevier.com/locate/talanta

Synchronous fluorescence determination of mercury ion with glutathione-capped CdS nanoparticles as a fluorescence probe

A.-Ni Liang, Lun Wang*, Hong-Qi Chen, Bin-Bin Qian, Bo Ling, Jie Fu

Anhui Key Laboratory of Chemo-Biosensing, College of Chemistry and Materials Science, Anhui Normal University, No. 1 Renmin Road, Wuhu 241000, PR China

ARTICLE INFO

Article history:
Received 5 September 2009
Received in revised form 9 December 2009
Accepted 13 December 2009
Available online 21 December 2009

Keywords:
Synchronous fluorescence
CdS nanoparticles
Probe
Hg^{2+} determination

ABSTRACT

Glutathione (GSH)-capped CdS nanoparticles was successfully synthesized in aqueous solutions at room temperature. Based on the characteristics of synchronous fluorescence spectroscopy (SFS), a simple method with high sensitivity and selectivity was developed for determination of Hg^{2+} with GSH-capped CdS nanoparticles as a fluorescence probe. The maximum synchronous fluorescence is located at 335 nm, scanning with excitation and emission wavelengths of 260 and 440 nm ($\Delta\lambda = \lambda_{em} - \lambda_{ex} = 180$ nm), respectively. Under optimal conditions, the quenched fluorescence intensity increased linearly with the concentration of Hg^{2+} ranging from 0.15×10^{-7} to 125×10^{-7} mol L^{-1}. The limit of detection was 4.5×10^{-9} mol L^{-1}. Compared with several fluorescence methods, the proposed method exhibited several merits in terms of its linear range and the sensitivity. The quenching mechanism was also discussed. Moreover, analytical application of the method was demonstrated by water samples.

1. Introduction

Heavy metal mercury is a hazardous contaminant of environment derived from both natural and industrial sources [1]. It has severe effects on the human health and environment even at very low concentration level [2,3]. Recently, Miyake et al. found that the very specific binding of the Hg^{2+} unexpectedly and significantly stabilizes naturally occurring thymine–thymine base mispairing in DNA duplexes [4]. Thus, effective determination of mercury is of great significance for environmental, biochemical science and medicine and the development of new methods for selective determination of mercury at ultra-trace levels is a challenging task. The advantages of fluorescence signaling in its intrinsic sensitivity have encouraged the development of a variety of fluorescent organic probes and sensors (organic dyes) for recognition and detection of mercury ion [5–7]. However, many of these small synthetic molecules lack water solubility and usually work in organic media (such as acetonitrile as solvent) [8], as well known, these organic solvent are harmful to environment. Furthermore, these conventional organic fluorescent dye molecules usually suffer from notorious limitations such as low signal intensities and photobleaching, and most of them tend to have narrow excitation spectra and often exhibit broad emission band with red tailing [9,10].

Colloidal semiconductor nanoparticles, often referred to as "quantum dots" (QDs), can overcome problems encountered by organic dye molecules. In recent years, QDs with water solubility and good photoluminescence stability become a new class of fluorescent probes for many biological applications [9,10]. Meanwhile, considerable efforts have also been focused on the development of a general sensing means, with QDs via analyte-induced fluorescence changes, for small molecules and ions [11]. Chen and Rosenzweig [12] demonstrated that the capping ligands have a profound effect on the fluorescence response of CdS QDs to different metal cations. Based on this, they gave the first example of Cu^{2+} and Zn^{2+} analysis by utilizing CdS QDs capped with different ligands in aqueous media. Moore and Patel [13] reported that the fluorescence intensity of aqueous CdS QDs was enhanced with introduction of selected Zn^{2+} and Cd^{2+} salts. Gatt'as-Asfura and Leblanc [14] synthesized the peptide-coated CdS QDs to develop a sensitive and selective sensing system for the detection of Cu^{2+} and Ag^{+}. Also, Xie et al. [15] modified CdSe–ZnS QDs with bovine serum albumin and used as fluorescence probe for Cu^{2+}.

CdS nanoparticles as a luminescence probe have attracted much attention [16]. However, most synthesis processes are costly, and require extreme reaction conditions. In addition, there are few reports on determination of Hg^{2+} by Synchronous fluorescence spectroscopy (SFS). SFS is a multidimensional fluorescence technique, which was described by Lloyd in 1971 [17] and was further developed with the aid of the Vo-Dinh theory [18]. This technique involves in scanning simultaneously by the excitation and emission monochromators. In the synchronous fluorescence spectra,

* Corresponding author. Tel.: +86 553 591008; fax: +86 553 5910008.
E-mail address: wanglun@mail.ahnu.edu.cn (L. Wang).

0039-9140/$ – see front matter © 2009 Elsevier B.V. All rights reserved.
doi:10.1016/j.talanta.2009.12.021

the sensitivity associated with general fluorescence is maintained while offering several advantages, e.g., simplification of emission spectra, improvement in the selectivity and spectral resolution because of the generally narrow spectral peaks, decreasing the interference due to light scattering. The aim of this paper is to synthesize GSH-capped CdS nanoparticles in aqueous solutions at room temperature, and to employ SFS for the determination of Hg^{2+} with GSH-capped CdS nanoparticles as a fluorescence probe.

2. Experimental

2.1. Apparatus and reagents

The synchronous fluorescence spectra were performed using a Hitachi F-4500 fluorescence spectrophotometer (Hitachi, Japan) equipped with a plotter unit and a quartz cell (1 cm × 1 cm), while fluorescence decay curves were performed with the time correlated single photo counting technique on the combined steady-state and lifetime spectrometer (Edinburgh Analytical Instruments, FLS920). The transmission electron microscopy (TEM) image of the nanoparticles was acquired on a Hitachi H-600 transmission electron microscope. All pH values were measured with a pHS-3C digital pH meter (Analytical Instruments Co., Tianda, Shanghai, China).

All chemicals were of analytical-reagent grade or better. The stock solutions of $CdCl_2{\cdot}2.5H_2O$ (Alfa, USA), thioacetamide (CH_3CSNH_2, Alfa), NaOH, $Hg(NO_3)_2$ (Shanghai Reagent Company, China), sodium hexametaphosphate and reduced glutathione (GSH) (Alfa) were prepared by dissolving them in doubly deionized water without further purification. The phosphoric buffer solution (PBS) was prepared by adjusting 0.067 mol L^{-1} KH_2PO_4 with 0.067 mol L^{-1} Na_2HPO_4. Water used throughout was doubly deionized.

2.2. Procedures

The colloidal solutions of CdS were prepared according to the scheme reported in the literatures [19,20]. Briefly, 200 mL 0.01 mol L^{-1} $CdCl_2{\cdot}2.5H_2O$ and 200 mL 0.01 mol L^{-1} CH_3CSNH_2 were mixed in a 500 mL three-necked round-bottomed flask and purged with N_2 for 20 min, then 20 mL of 0.1 mol L^{-1} sodium hexametaphosphate as the stabilizing agent were added into the mixture under vigorous stirring, and the pH was adjusted to 8.0 using 0.1 mol L^{-1} NaOH solutions. After 90 min, certain amount GSH were added into the as-prepared CdS solutions and the GSH-capped CdS nanoparticles were obtained in 30 min.

In a series of 10 mL volumetric flasks, 700 μL of as-prepared functional CdS solution, 1 mL of PBS (pH 7.0), and various amount of Hg^{2+} were added, then the mixture was diluted to the mark with water and mixed thoroughly. At room temperature (25 ± 2 °C), the mixture was transferred for measurements after 5 min. The synchronous fluorescence spectra of functional CdS nanoparticles in the absence and presence of Hg^{2+} were measured at λ = 335 nm when Δλ = 180 nm (scanning with excitation and emission wavelengths of 260 and 440 nm, respectively).

3. Results and discussions

3.1. TEM image of CdS nanoparticles

The morphology of CdS nanoparticles was studied by TEM (Fig. 1). The typical TEM image shows that the shape of these nanoparticles is irregular, monodisperse, with the average size about 20 nm. The solublization and cross-linking steps did not result in aggregation. In addition, GSH-capped CdS nanoparticles can be stably dispersed in water more for 2 months without significant precipitation in the dark, under about 4 °C.

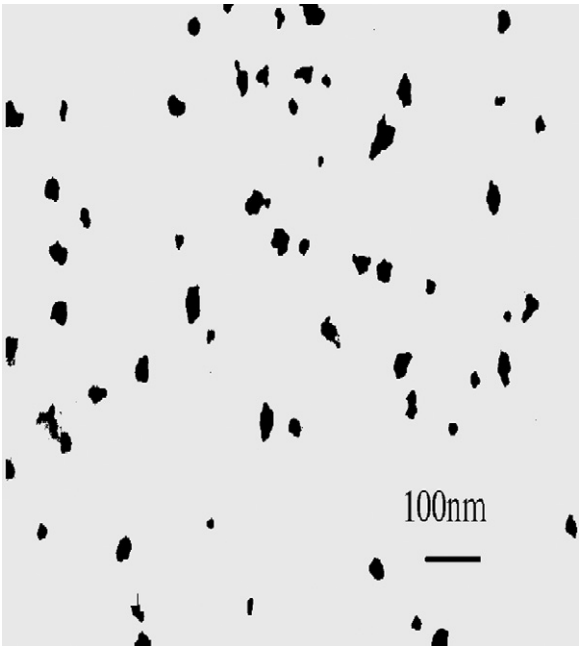

Fig. 1. TEM image of CdS nanoparticles.

3.2. Fluorescence characteristic of the GSH-capped CdS–Hg^{2+} system

The synchronous fluorescence spectra of GSH-capped CdS in the presence of various Hg^{2+} concentrations are shown in Fig. 2. When Δλ = 180 nm (scanning with excitation and emission wavelengths of 260 and 440 nm, respectively), the synchronous fluorescence peak of GSH-capped CdS is located at 335 nm. Furthermore, the maximum fluorescence intensity of GSH-capped CdS was significantly quenched with increase of Hg^{2+} concentration. The phenomena indicated that the SFS could be a feasible method for the determination of Hg^{2+}.

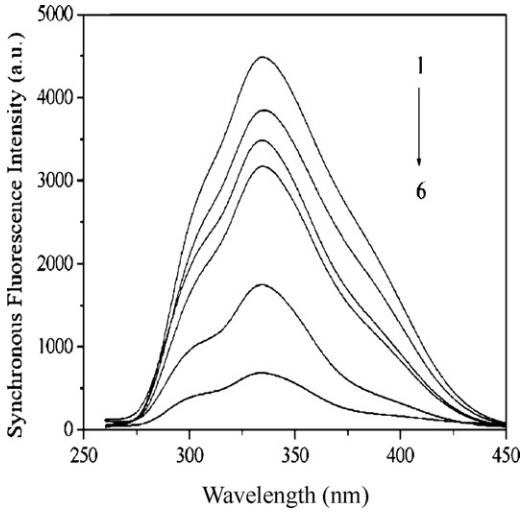

Fig. 2. The synchronous fluorescence spectra of GSH-capped CdS with different concentrations of Hg^{2+}. From 1 to 6: 0, 0.4, 2.0, 3.5, 25, and 100 × 10^{-7} mol L^{-1} Hg^{2+}; GSH-capped CdS, 3.5 × 10^{-4} mol L^{-1}; pH, 7.0; $\lambda_{em} - \lambda_{ex}$ = 440–260 nm; slit widths, ex/em = 10 nm/10 nm; PMT voltage, 700 V.

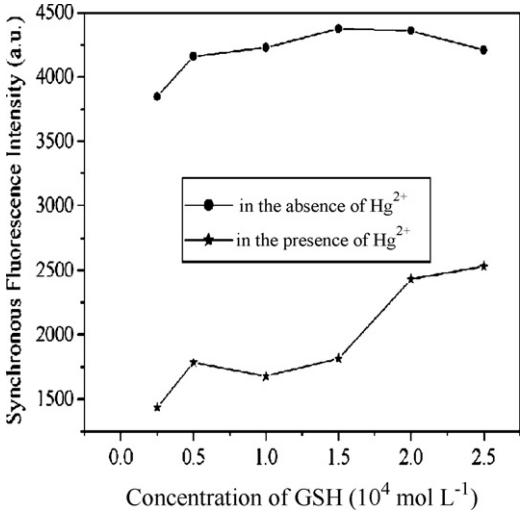

Fig. 3. Effect of the concentration of GSH. Hg^{2+}, 5×10^{-7} mol L^{-1}.

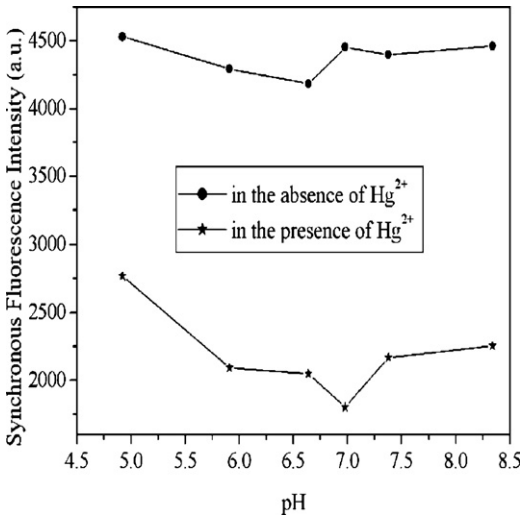

Fig. 4. Effect of pH. Hg^{2+}, 5×10^{-7} mol L^{-1}; GSH-capped CdS, 3.5×10^{-4} mol L^{-1}.

3.3. Reaction and mixing sequence

According to the experimental results, the reaction between GSH-capped CdS and Hg^{2+} reached the equilibrium very quickly within 5 min, and the relative synchronous fluorescence signals were stable for at least 60 min at room temperature (25 ± 2 °C). In addition, after investigating several mixing sequences, we discovered that the best order is to mix GSH-capped CdS and PBS first, and then Hg^{2+}. Therefore, all the measurements were made after GSH-capped CdS, PBS and Hg^{2+} were completely mixed for 5 min.

3.4. Effect of the concentration of GSH

GSH, as an important tripeptide with strong affinity to cadmium, is very suitable to modify CdS nanoparticles and the properties of GSH-capped CdS complexes have been reported before [21]. Modified by GSH, the optical stability of CdS is improved, as well exhibits an advantage to interact with Hg^{2+}. Hg^{2+}, for being a "soft" metal cation, prefers to strong affinity to RSH and RS^- compounds. The effect of the concentration of GSH on the synchronous fluorescence intensity of the studied system was shown in Fig. 3. The maximum difference of synchronous fluorescence intensity changed slightly when the concentration of GSH was in the range of 1.0×10^{-4} to 1.5×10^{-4} mol L^{-1}. In order to get a high sensitivity, the concentration of 1.0×10^{-4} mol L^{-1} GSH was recommended in this assay.

3.5. Effect of pH

The effect of pH on the determination of Hg^{2+} in a range from 4.9 to 8.3 was studied (as shown in Fig. 4). It can be found that pH values have little influence on the signal measured and the maximum difference of the synchronous fluorescence intensity occurred at pH 7.0. In addition, different buffers were also tested and the results showed that PBS was the best suited. So in the experiment, 1 mL of pH 7.0 PBS was used.

3.6. Effect of the concentration of GSH-capped CdS

The effect of the GSH-capped CdS concentration on the synchronous fluorescence intensity in the presence of Hg^{2+} was also investigated (as shown in Fig. 5). With increasing concentration of GSH-capped CdS, the fluorescence intensity difference of the system increased. However, the relative intensities increased very slightly after the concentration of GSH-capped CdS reached 3.0×10^{-4} mol L^{-1} (referring to Cd^{2+}) and it dropped when GSH-capped CdS reached 4.0×10^{-4} mol L^{-1}. For a compromise between the sensitivity and the linear range of the calibration function, 3.5×10^{-4} mol L^{-1} is selected for further research.

3.7. Effect of potential interfering ions

The effect of typical potential interfering cations on the fluorescence intensity of GSH-capped CdS was studied. As shown in Fig. 6, it could be easily found that the synchronous fluorescence intensity of GSH-capped CdS was insensitive to most metal cations, while Hg^{2+} has a strong quenching effect. 2000-Fold Na^+ and K^+ showed no interference for the determination of Hg^{2+}. Some potential interfering ions in water samples, such as Co^{2+}, Pb^{2+}, I^-, and Mn^{2+} caused a slight effect on the fluorescence intensity of GSH-capped CdS. On the other hand, Zn^{2+} exhibited a positive quenching of fluorescence intensity, which is consistent with the previous reports [13,22,23]. In the experiments, Cu^{2+} was the major interference when in the presence of 10-fold excesses, so a proper amount of thiourea solutions can be added as masking agents [24]. Briefly, the proposed method showed a relative specific quenching effect of Hg^{2+}.

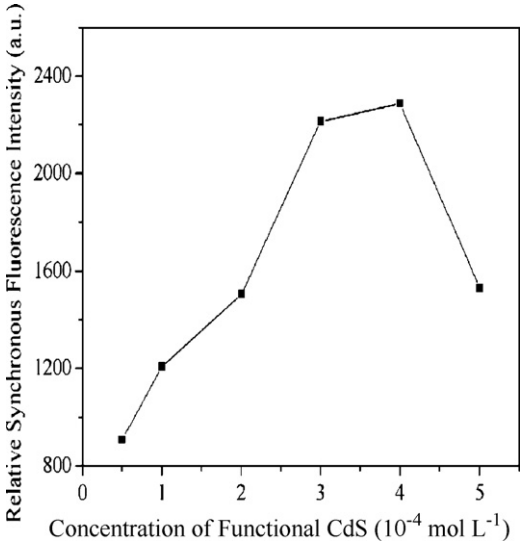

Fig. 5. Effect of the concentration of GSH-capped CdS.

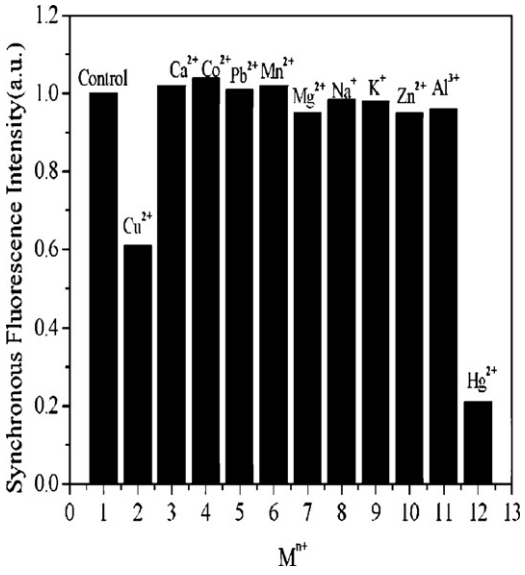

Fig. 6. Effect of potential interfering ions. Hg^{2+}, 25×10^{-7} mol L^{-1}; 2000-fold K^+ and Na^+; 200-fold Mg^{2+} and Ca^{2+}; 75-fold Al^{3+}; 50-fold Pb^{2+} and Mn^{2+}; 40-fold Zn^{2+} and Co^{2+}; 10-fold Cu^{2+}; 180-fold F^-; 120-fold Br^- and I^-; 60-fold CO_3^{2-}.

3.8. Quenching mechanism

Several mechanisms have been proposed to explain how ions quench fluorescence intensity of nanoparticles, including inner filter effects, non-radiative recombination pathways, electron transfer process and ion-binding type [14,25]. Chen et al. [26,27,4] thought the fluorescence quenching with no spectra shift by Hg^{2+} can be understood due to facilitating non-radiative e^-/h^+ recombination anniliation on the surface of QDs through a effective electron transfer process between surface functional amide groups $-NH_2$ and Hg^{2+}. However, a blue-shift on the general fluorescence spectra was observed in our experiments (Fig. 7). Meanwhile, the fluorescence lifetimes of GSH-capped CdS were quenched with increasing of Hg^{2+} concentration, and the decays of all the samples were multiexponential and fitted using the third-order equation (as shown in Fig. 8 and Table 1), which may result from the ultrafast electron transfer from CdS nanoparticles to Hg^{2+} [28]. Isarov and Chrysochoos [29] investigated Cu^{2+} in quenching the emission of CdS

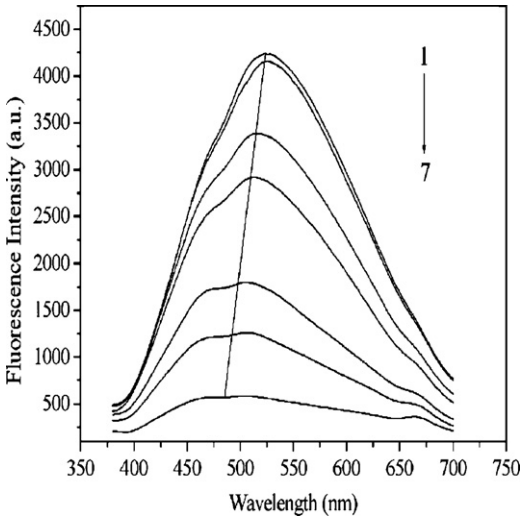

Fig. 7. The general fluorescence spectra of GSH-capped CdS with different concentrations of Hg^{2+}. From 1 to 7: 0, 0.25, 2.5, 5.0, 25, 50, and 100×10^{-7} mol L^{-1} Hg^{2+}.

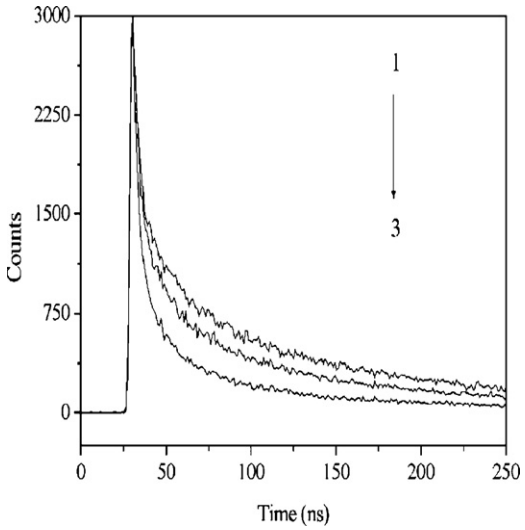

Fig. 8. Fluorescence decay curves (λ_{ex} = 340 nm) of GSH-capped CdS with different concentrations of Hg^{2+}. From 1 to 3: 0, 40, and 100×10^{-7} mol L^{-1} Hg^{2+}.

QDs. They found that some ultrasmall Cu*x*S (*x* = 1, 2) particles could form on the surface of CdS nanoparticles. In our case, one should also be aware that the K_{sp} of HgS ($K_{sp} = 1.6 \times 10^{-52}$) ($K_{sp}$ stands for solubility product constant) is much lower than that of CdS ($K_{sp} = 8 \times 10^{-27}$), resulting in a chemical displacement of surface Cd^{2+} by Hg^{2+} to form some ultra small HgS particles on the surface of CdS, as described in a previous report [30]. The latter effect may play a leading role in explaining fluorescence quenching. For these structure, electron and hole transfer from the CdS to the HgS energy level is assumed to be much faster than the process of fluorescence generation in the CdS, the energy of electrons are released in non-radioactive form. This is also much similar to the case of CuSe on CdSe [15,31].

3.9. Analytical performance

Under the optimal conditions, it was found that Hg^{2+} quenched the synchronous fluorescence intensity of GSH-capped CdS in a concentration dependence that is best described by a Stern–Volmer equation:

$$\frac{I_{SF0}}{I_{SF}} = 1 + K_{sv}[Q]$$

where I_{SF} and I_{SF0} are the synchronous fluorescence intensity of the GSH-capped CdS at a given Hg^{2+} concentration and in a Hg^{2+}-free solution, K_{sv} is the Stern–Volmer quenching constant and [*Q*] is the concentration of Hg^{2+}. The calibration plot of I_{SF0}/I_{SF} with Hg^{2+} concentration is linear ranging from 0.15×10^{-7} to 125×10^{-7} mol L^{-1} with a correlation coefficient (*R*) of 0.9984 (see Fig. 9). K_{sv} was found to be 0.52×10^6 L mol^{-1}. The limit of detection (LOD), calculated by the equation LOD = $3S_b/K$, where S_b is the standard deviation of blank measurements (*n* = 7) and *K* is the slope of calibration graph, was 4.5×10^{-9} mol L^{-1}. The relative standard deviations of seven

Table 1
The fit results of fluorescence lifetimes before and after quenching of GSH-capped CdS.

Quenched by Hg^{2+} ($\times 10^{-7}$ mol L^{-1})	τ (1/ns)	τ (2/ns)	τ (3/ns)	χ^2
0	8.42	59.52	216.35	1.046
40	6.73	46.08	190.57	1.048
100	5.83	37.41	183.63	1.20

Table 2
Comparison of the main characteristics for fluorimetric determination of Hg^{2+} with several reagents.

Reagent[a]	$\lambda_{ex}/\lambda_{em}$ (nm)	Linear range ($\times 10^{-7}$ mol L^{-1})	LOD ($\times 10^{-9}$ mol L^{-1})
AnthBT [5]	368/418	0.75–10	58
BBA [32]	340/380	0.1–1.0	10
Iodid and ferroin [6]	320/509	0.32–9.5	6.2
MAA-capped InP QDs [33]	750/826	25–398	997
Cys-capped CdS QDs [34]	360/495	0.16–1.12	2.4
This work	$\Delta\lambda$ = 180 nm	0.15–125	4.5

[a] The abbreviation of the reagents represented as follows: AnthBT, *N*-9-anthrylmethyl-*N*-methyl-*N*0-benzoylthiourea; BBA, binaphthyl-based amphiphiles; MAA-capped InP QDs, mercaptoacetic acid-capped InP QDs; Cys-capped CdS QDs, L-Cysteine-capped CdS QDs; dBSA-coated CdTe QDs, denatured BSA-coated CdTe QDs.

Table 3
Analytical results for the determination of Hg^{2+} in water samples.

Samples	Hg^{2+} added (nmol L^{-1})	Hg^{2+} found[a] (nmol L^{-1})	Found by ETAAS (nmol L^{-1})
Underground water[b]	80.0	85.3 ± 1.3	84.5
Lake water[c]	50.0	57.5 ± 0.7	58.7
	100.0	111.6 ± 2.2	112.7
River water[d]	0.0	55.7 ± 1.3	55.2
	50.0	103.2 ± 1.8	102.4
Synthetic Hg^{2+}-polluted water[e]	0.0	98.5 ± 1.5	97.3
	50.0	147.1 ± 2.3	146.8

[a] Mean of five experiments ± standard deviation.
[b] Underground water at HHP, Wuhu.
[c] Lake water at JH, Wuhu.
[d] River water at EDA, Wuhu.
[e] Synthesized by: 100 nmol L^{-1} $Hg(NO_3)_2$, 200 nmol L^{-1} $MnSO_4$, 1 μmol L^{-1} $AlCl_3$, 20 nmol L^{-1} $NiSO_4$, 5 μmol L^{-1} $Pb(NO_3)_2$, 3 nmol L^{-1} $CuSO_4$, 50 μmol L^{-1} $MgCl_2$ and $CaCl_2$.

replicate measurements for 2.5×10^{-8} and 2.5×10^{-6} mol L^{-1} were 2.5 and 1.5%, respectively.

For comparative purpose, some main characteristics of other reagents for Hg^{2+} determination are summarized in Table 2. It can be found that some organic dye probes, such as AnthBT [5] and BBA [32] are either toxic or difficult to synthesis. Meanwhile, they have smaller Stokes' shift and narrow linear range. In contrast, some QDs are more sensitive fluorescence reagents for Hg^{2+}determination. However, from the analytical performances, it is obvious that the method is of a wider linear range and much more simple than most of current used and prescribed method.

To test the applicability of the proposed method, it was applied to the determination of Hg^{2+} in water samples, which were filtered four times through qualitative filter paper before use. The real samples (underground water and lake water) showed that Hg^{2+} almost was not present in them, so they were analyzed using the standard addition method according to the procedure described above. The determination results were presented in Table 3. It can be found these measured values are in agreement with those obtained by electrothermal atomic absorption spectrometry (ETAAS).

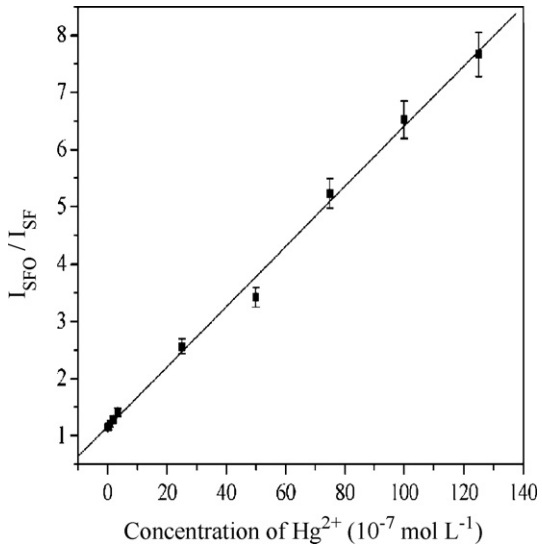

Fig. 9. The Stern–Volmer curve of synchronous fluorescence method for determination of Hg^{2+}. Error bars (relative error = 5%).

4. Conclusion

A simple synchronous fluorescence spectroscopy was successfully constructed for sensitive and selective determination of Hg^{2+} in aqueous solution with GSH-capped CdS nanoparticles as a fluorescence probe. Compared with organic fluorescent probes, the method offers many merits, such as high sensitivity, large Stoke's shift ($\Delta\lambda$ = 180 nm), low cost and simple preparation. Based on the strong quenching effect of analyte, a very good linear relationship was observed in a Hg^{2+} concentration ranging from 0.15×10^{-7} to 125×10^{-7} mol L^{-1}. What is more, the feasibility of the synchronous fluorescence spectroscopy as a promising approach in fluorometric metal ion analysis has been demonstrated.

Acknowledgements

This work was supported by Natural Science Foundation of China (20875004).

References

[1] N.N. Green, A. Earn Shaw, Chemistry of Elements, Pergamon Press, New York, 1984.
[2] Y.K. Yang, K.J. Yook, J.S. Tae, J. Am. Chem. Soc. 127 (2005) 16760–16761.
[3] R.H. Yang, W.H. Chan, A.W.M. Lee, P.F. Xia, H.K. Zhang, K.A. Li, J. Am. Chem. Soc. 125 (2003) 2884–2885.
[4] Y. Miyake, H. Togashi, M. Tashiro, H. Yamaguchi, S.J. Oda, M. Kudo, Y. Tanaka, Y. Kondo, R. Sawa, T. Fujimoto, T. Machinami, A. Ono, J. Am. Chem. Soc. 128 (2006) 2172–2173.
[5] M.S. Ïandor, F. Geistmann, M. Schuster, Anal. Chim. Acta 388 (1999) 19–26.
[6] M.S. Hosseini, M.H. Hashemi, Anal. Sci. 20 (2004) 1449–1452.
[7] E.M. Nolan, S.J. Lippard, J. Am. Chem. Soc. 125 (2003) 14270–14271.

[8] K. Rurack, U. Resch-Genger, J.L. Bricks, M. Spieles, Chem. Commun. 21 (2000) 2103–2104.
[9] M. Bruchez Jr., M. Moronne, P. Gin, S. Weiss, A.P. Alivisatos, Science 281 (1998) 2013–2016.
[10] W.C.W. Chan, S. Nie, Science 281 (1998) 2016–2018.
[11] J.M. Costa-Fernández, R. Pereiro, A. Sanz-Medel, TrAC, Trends Anal. Chem. 25 (2006) 207–218.
[12] Y.F. Chen, Z. Rosenzweig, Anal. Chem. 74 (2002) 5132–5138.
[13] D.E. Moore, K. Patel, Langmuir 17 (2001) 2541–2544.
[14] K.M. Gattás-Asfura, R.M. Leblanc, Chem. Commun. 21 (2003) 2684–2685.
[15] H.Y. Xie, J.G. Liang, Z.L. Zhang, Y. Liu, Z.K. He, D.W. Pang, Spectrochim. Acta A 60 (2004) 2527–2530.
[16] R.C. Somers, M.G. Bawendi, D.G. Nocera, Chem. Soc. Rev. 36 (2007) 579–591.
[17] J.B.F. Lloyd, Nature 231 (1971) 64–67.
[18] T. Vo-Dinh, Anal. Chem. 50 (1978) 396–401.
[19] H. Liu, W.Y. Li, H.Z. Yin, X.W. He, L.X. Chen, Acta Chim. Sinica 63 (2005) 301–306.
[20] L. Wang, Y. Liu, H.Q. Chen, A.N. Liang, F.G. Xu, Chin. Chem. Lett. 18 (2007) 369–372.
[21] W. Bae, R.K. Mehra, J. Inorg. Biochem. 69 (1998) 33–43.
[22] L. Spanhel, M. Haase, H. Weller, A. Henglein, J. Am. Chem. Soc. 109 (1987) 5649–5655.
[23] K. Sooklal, B.S. Cullum, A.S. Mngel, C.J. Murphy, J. Phys. Chem. 100 (1996) 4551–4555.
[24] Q.G. Liao, Y.F. Li, C.Z. Huang, Talanta 71 (2007) 567–572.
[25] B. Chen, P. Zhong, Anal. Bioanal. Chem. 381 (2005) 986–992.
[26] J.L. Chen, Y.C. Gao, Z.B. Xu, G.H. Wu, Y.C. Chen, C.Q. Zhu, Anal. Chim. Acta 577 (2006) 77–84.
[27] M.Y. Chae, A.W. Czarmik, J. Am. Chem. Soc. 114 (1992) 9704–9705.
[28] R. van Beek, A.P. Zoombelt, L.W. Jenneskens, C.A. vanWalree, C. de Mello Donegá, D. Veldman, R.A.J. Janssen, Chem. Eur. J. 12 (2006) 8075–8083.
[29] A.V. Isarov, J. Chrysochoos, Langmuir 13 (1997) 3142–3149.
[30] A. Hiisselbartb, A. EychmiiUer, R. Eicbberger, M. Giersig, A. Mews, H. Weller, J. Phys. Chem. 97 (1993) 5333–5340.
[31] M.T. Fernández-Argüelles, W.J. Jin, J.M. Costa-Fernández, R. Pereiro, A. Sanz-Medel, Anal. Chim. Acta 549 (2005) 20–25.
[32] B. Juskowiak, Anal. Chim. Acta 320 (1996) 115–124.
[33] C.Q. Zhu, L. Li, F. Fang, J.L. Chen, Y.Q. Wu, Chem. Lett. 34 (2005) 898–899.
[34] Z.X. Cai, H. Yang, Y. Zhang, X.P. Yan, Anal. Chim. Acta 559 (2006) 234–239.